Japan J. Indust. Appl. Math. (2016) 33:121–143
DOI 10.1007/s13160-015-0196-2

ORIGINAL PAPER

Area 2

A genuinely stable Lagrange–Galerkin scheme for convection-diffusion problems

Masahisa Tabata[1] · **Shinya Uchiumi**[2,3]

Received: 18 April 2015 / Revised: 16 October 2015 / Published online: 3 November 2015

Abstract We present a Lagrange–Galerkin scheme free from numerical quadrature for convection-diffusion problems. Since the scheme can be implemented exactly as it is, theoretical stability result is assured. While conventional Lagrange–Galerkin schemes may encounter the instability caused by numerical quadrature error, the present scheme is genuinely stable. For the P_k-element we prove error estimates of $O(\Delta t + h^2 + h^{k+1})$ in $\ell^\infty(L^2)$-norm and of $O(\Delta t + h^2 + h^k)$ in $\ell^\infty(H^1)$-norm. Numerical results reflect these estimates.

Keywords Lagrange–Galerkin scheme · Finite element method · Convection-diffusion problems · Exact integration

Mathematics Subject Classification 65M12 · 65M25 · 65M60 · 76M10

1 Introduction

The Lagrange–Galerkin method, which is also called characteristics finite element method or Galerkin-characteristics method, is a powerful numerical method for flow problems such as the convection-diffusion equations and the Navier–Stokes equations.

✉ Masahisa Tabata
tabata@waseda.jp

Shinya Uchiumi
su48@fuji.waseda.jp

1 Department of Mathematics, Waseda University, 3-4-1, Ohkubo, Shinjuku, Tokyo 169-8555, Japan

2 Graduate School of Fundamental Science and Engineering, Waseda University, 3-4-1, Ohkubo, Shinjuku, Tokyo 169-8555, Japan

3 Research Fellow of Japan Society for the Promotion of Science, Tokyo, Japan

In this method the material derivative is discretized along the characteristic curve, which originates the robustness for convection-dominated problems. Although, as a result of the discretization along the characteristic curve, a composite function term at the previous time appears, it is converted to the right-hand side in the system of the linear equations. Thus, the coefficient matrix in the left-hand side is symmetric, which allows us to use efficient linear solvers for symmetric matrices such as the conjugate gradient method and the minimal residual method [2,15].

Stability and error analysis of LG schemes has been done in [1,3,4,6,9–14,16]; see also the bibliography therein. Pironneau [11] analyzed convection-diffusion problems and the Navier–Stokes equations to obtain suboptimal convergence results. Optimal convergence results were obtained by Douglas-Russell [6] for convection-diffusion problems and by Süli [16] for the Navier–Stokes equations. Optimal convergence results of second order in time were obtained by Boukir et al. [4] for the Navier–Stokes equations in multi-step method and by Rui-Tabata [14] for convection-diffusion problems in single-step method. All these theoretical results are derived under the condition that the integration of the composite function term is computed exactly. Since, in real problems, it is difficult to get the exact integration value, numerical quadrature is usually employed. It is, however, reported that instability may occur caused by numerical quadrature error in [9,17,18]. That is, the theoretical stability results may collapse by the introduction of numerical quadrature.

Several methods have been studied to avoid the instability. The map of a particle from a time to the previous time along the trajectory, which is nothing but to solve a system of ordinary differential equations (ODEs), is simplified in [3,9,13]. Morton-Priestley-Suli [9] solved the ODEs only at the centroids of the elements, and Priestley [13] did only at the vertices of the elements. The map of the other points is approximated by linear interpolation of those values. It becomes possible to perform the exact integration of the composite function term with the simplified map. Bermejo-Saavedra [3] used the same simplified map as [13] to employ a numerical quadrature of high accuracy to the composite function term. Tanaka-Suzuki-Tabata [19] approximated the map by a locally linearized velocity and the backward Euler approximation for the solution of the ODEs in P_1-element. The approximate map makes possible the exact integration of the composite function term with the map. Pironneau-Tabata [12] used mass lumping in P_1-element to develop a scheme free from quadrature for convection-diffusion problems.

In this paper we prove the stability and convergence for the scheme with the same approximate map as [19] in P_k-element for convection-diffusion problems. Since we neither solve the ODEs nor use numerical quadrature, our scheme can be precisely implemented to realize the theoretical results. It is, therefore, a genuinely stable Lagrange–Galerkin scheme. Our convergence results are of $O(\Delta t + h^2 + h^{k+1})$ in $\ell^\infty(L^2)$-norm and of $O(\Delta t + h^2 + h^k)$ in $\ell^\infty(H^1)$-norm. They are best possible in both norms for P_1-element and in $\ell^\infty(H^1)$-norm for P_2-element

The contents of this paper are as follows. In the next section we describe the convection-diffusion problem and some preparation. In Sect. 3, after recalling the conventional Lagrange–Galerkin scheme, we present our genuinely stable Lagrange–Galerkin scheme. In Sect. 4 we show stability and convergence results, which are

proved in Sect. 5. In Sect. 6 we show some numerical results, which reflect the theoretical convergence order. In Sect. 7 we give conclusions.

2 Preliminaries

We state the problem and prepare notation used throughout this paper.

Let Ω be a polygonal or polyhedral domain of $\mathbb{R}^d$ $(d = 2, 3)$ and $T > 0$ be a time. We use the Sobolev spaces $L^p(\Omega)$ with the norm $\|\cdot\|_{0,p}$, $W^{s,p}(\Omega)$ and $W_0^{s,p}(\Omega)$ with the norm $\|\cdot\|_{s,p}$ and the semi-norm $|\cdot|_{s,p}$ for $1 \le p \le \infty$ and a positive integer s. We will write $H^s(\Omega) = W^{s,2}(\Omega)$ and drop the subscript $p = 2$ in the corresponding norms. The L^2-norm $\|\cdot\|_0$ is simply denoted by $\|\cdot\|$. The dual space of $H_0^1(\Omega)$ is denoted by $H^{-1}(\Omega)$. For the vector-valued function $w \in W^{1,\infty}(\Omega)^d$ we define the semi-norm $|w|_{1,\infty}$ by

$$\left\| \left\{ \sum_{i,j=1}^{d} \left(\frac{\partial w_i}{\partial x_j} \right)^2 \right\}^{1/2} \right\|_{0,\infty}.$$

The parenthesis $(\cdot, \cdot)$ shows the L^2-inner product $(f, g) \equiv \int_\Omega fg \, dx$. For a Sobolev space $X(\Omega)$ we use abbreviations $H^m(X) = H^m(0, T; X(\Omega))$ and $C(X) = C([0, T]; X(\Omega))$. We define a function space $Z^m(t_1, t_2)$ by

$$Z^m(t_1, t_2) \equiv \{ f \in H^j(t_1, t_2; H^{m-j}(\Omega)); \ j = 0, \dots, m, \ \|f\|_{Z^m(t_1,t_2)} < \infty \},$$

$$\|f\|_{Z^m(t_1,t_2)} \equiv \left\{ \sum_{j=0}^{m} \|f\|^2_{H^j(t_1,t_2;H^{m-j})} \right\}^{1/2}$$

and denote $Z^m(0, T)$ by Z^m.

We consider the convection-diffusion problem: find $\phi : \Omega \times (0, T) \to \mathbb{R}$ such that

$$\frac{\partial \phi}{\partial t} + u \cdot \nabla \phi - \nu \Delta \phi = f, \qquad (x, t) \in \Omega \times (0, T), \tag{1a}$$

$$\phi = 0, \qquad (x, t) \in \partial\Omega \times (0, T), \tag{1b}$$

$$\phi = \phi^0, \qquad x \in \Omega, \ t = 0, \tag{1c}$$

where $\partial\Omega$ is the boundary of Ω and $\nu > 0$ is a diffusion constant which is less than or equal to a given ν_0. Functions $u : \Omega \times (0, T) \to \mathbb{R}^d$, $f \in C(L^2)$ and $\phi^0 \in C(\bar{\Omega})$ are given.

Remark 1 As usual, in place of (1b), we can deal with the inhomogeneous boundary condition $\phi = g$ by replacing the unknown function ϕ by $\widetilde{\phi} \equiv \phi - \widetilde{g}$ if the function g defined on $\partial\Omega \times (0, T)$ can be extended to a function $\widetilde{g}$ in $\Omega \times (0, T)$ appropriately.

Let $\Delta t > 0$ be a time increment, $N_T \equiv \lfloor T/\Delta t \rfloor$, $t^n \equiv n\Delta t$ and $\psi^n \equiv \psi(\cdot, t^n)$ for a function ψ defined in $\Omega \times (0, T)$. For a set of functions $\psi = \{\psi^n\}_{n=0}^{N_T}$, two norms

$\|\cdot\|_{\ell^\infty(L^2)}$ and $\|\cdot\|_{\ell^2(n_1,n_2;L^2)}$ are defined by

$$\|\psi\|_{\ell^\infty(L^2)} \equiv \max\left\{\left\|\psi^n\right\|; n = 0, \ldots, N_T\right\},$$
$$\|\psi\|_{\ell^2(n_1,n_2;L^2)} \equiv \left(\Delta t \sum_{n=n_1}^{n_2} \left\|\psi^n\right\|^2\right)^{1/2}$$

and denote $\|\psi\|_{\ell^2(1,N_T;L^2)}$ by $\|\psi\|_{\ell^2(L^2)}$.

Let u be smooth. The characteristic curve $X(t;x,s)$ is defined by the solution of the system of the ordinary differential equations,

$$\frac{dX}{dt}(t;x,s) = u(X(t;x,s),t), \quad t < s, \tag{2a}$$
$$X(s;x,s) = x. \tag{2b}$$

Then, we can write the material derivative term $\frac{\partial\phi}{\partial t} + u\cdot\nabla\phi$ as

$$\left(\frac{\partial\phi}{\partial t} + u\cdot\nabla\phi\right)(X(t),t) = \frac{d}{dt}\phi(X(t),t).$$

For $w : \Omega \to \mathbb{R}^d$ we define the mapping $X_1(w) : \Omega \to \mathbb{R}^d$ by

$$(X_1(w))(x) \equiv x - w(x)\Delta t. \tag{3}$$

Remark 2 The image of x by $X_1(u(\cdot,t))$ is nothing but the backward Euler approximation of $X(t-\Delta t;x,t)$.

The symbol $\circ$ stands for the composition of functions, e.g., $(g\circ f)(x) \equiv g(f(x))$.

Let $\mathcal{T}_h \equiv \{K\}$ be a triangulation of $\bar{\Omega}$ and $h \equiv \max_{K\in\mathcal{T}_h} \mathrm{diam}(K)$ be the maximum element size. Throughout this paper we consider a regular family of triangulations $\{\mathcal{T}_h\}_{h\downarrow 0}$. Let k be a fixed positive integer and $V_h \subset H_0^1(\Omega)$ be the P_k-finite element space,

$$V_h \equiv \{v_h \in C(\bar{\Omega}) \cap H_0^1(\Omega);\ v_{h|K} \in P_k(K),\ \forall K \in \mathcal{T}_h\},$$

where $P_k(K)$ is the set of polynomials on K whose degrees are less than or equal to k. Let $\widehat{\phi}_h \in V_h$ be the Poisson projection of $\phi \in H_0^1(\Omega)$ defined by

$$(\nabla(\widehat{\phi}_h - \phi), \nabla\psi_h) = 0, \quad \forall\psi_h \in V_h. \tag{4}$$

We use c to represent a generic positive constant independent of h, Δt, ν, f and ϕ which may take different values at different places. The notation $c(A)$ means that c depends on a positive parameter A and that c increases monotonically when A increases. The constants c_0, c_1 and c_2 stand for $c_0 = c(\|u\|_{C(L^\infty)}), c_1 = c(\|u\|_{C(W^{1,\infty})})$ and $c_2 = c(\|u\|_{C(W^{2,\infty})})$. We also use fixed positive constants α_* and δ_* defined in Lemma 1 in the next section and in Lemma 5 in Sect. 5, respectively.

3 A genuinely stable Lagrange–Galerkin scheme

The conventional Lagrange–Galerkin scheme, which we call Scheme LG, is described as follows.

Scheme LG Let $\phi_h^0 = \widehat{\phi}_h^0$. Find $\{\phi_h^n\}_{n=1}^{N_T} \subset V_h$ such that for $n = 1, \ldots, N_T$

$$\left(\frac{\phi_h^n - \phi_h^{n-1} \circ X_1^n}{\Delta t}, \psi_h \right) + \nu(\nabla \phi_h^n, \nabla \psi_h) = (f^n, \psi_h), \quad \forall \psi_h \in V_h, \tag{5}$$

where $X_1^n = X_1(u^n)$.

For this scheme error estimates

$$\begin{aligned} &\|\phi_h - \phi\|_{\ell^\infty(L^2)} \le c(h^k + \Delta t),\ c(1/\nu)(h^{k+1} + \Delta t), \\ &\|\phi_h - \phi\|_{\ell^\infty(H^1)} \le c(1/\nu)(h^k + \Delta t) \end{aligned} \tag{6}$$

are proved in [6], where the composite function term $(\phi_h^{n-1} \circ X_1^n, \psi_h)$ is assumed to be exactly integrated.

Although the function ϕ_h^{n-1} is a polynomial on each element K, the composite function $\phi_h^{n-1} \circ X_1^n$ is not a polynomial on K in general since the image $X_1^n(K)$ of an element K may spread over plural elements. Hence, it is hard to calculate the composite function term $(\phi_h^{n-1} \circ X_1^n, \psi_h)$ exactly. In practice, the following numerical quadrature has been used. Let $g : K \to \mathbb{R}$ be a continuous function. A numerical quadrature $I_h[g; K]$ of $\int_K g\, dx$ is defined by

$$I_h[g; K] \equiv \mathrm{meas}(K) \sum_{i=1}^{N_q} w_i\ g(a_i), \tag{7}$$

where N_q is the number of quadrature points and $(w_i, a_i) \in \mathbb{R} \times K$ is a pair of weight and point for $i = 1, \ldots, N_q$. We call the practical scheme using numerical quadrature Scheme LG′.

Scheme LG′ Let $\phi_h^0 = \widehat{\phi}_h^0$. Find $\{\phi_h^n\}_{n=1}^{N_T} \subset V_h$ such that for $n = 1, \ldots, N_T$

$$\begin{aligned} \frac{1}{\Delta t}(\phi_h^n, \psi_h) - \frac{1}{\Delta t} \sum_{K \in \mathcal{T}_h} I_h[(\phi_h^{n-1} \circ X_1^n)\psi_h; K] + \nu(\nabla \phi_h^n, \nabla \psi_h) \\ = (f^n, \psi_h), \quad \forall \psi_h \in V_h, \end{aligned} \tag{8}$$

where $X_1^n = X_1(u^n)$.

It is reported that the results (6) do not hold for Scheme LG′ [9,17–19].

We denote by $\Pi_h^{(1)}$ the Lagrange interpolation operator to the P_1-finite element space. The following lemma is well-known [5].

Lemma 1 *(i) There exists a positive constant c_Π such that for $w \in W^{2,\infty}(\Omega)^d$*

$$\|\Pi_h^{(1)} w - w\|_{0,\infty} \le c_\Pi h^2 \, |w|_{2,\infty} .$$

(ii) There exists a positive constant $\alpha_* \ge 1$ such that for $w \in W^{1,\infty}(\Omega)^d$

$$|\Pi_h^{(1)} w|_{1,\infty} \le \alpha_* \, |w|_{1,\infty} .$$

We now present our genuinely stable scheme GSLG, which is free from quadrature and exactly computable. We define a locally linearized velocity u_h and a mapping X_{1h}^n by

$$u_h \equiv \Pi_h^{(1)} u, \quad X_{1h}^n \equiv X_1(u_h^n).$$

Scheme GSLG Let $\phi_h^0 = \widehat{\phi}_h^0$. Find $\{\phi_h^n\}_{n=1}^{N_T} \subset V_h$ such that for $n = 1, \ldots, N_T$

$$\left(\frac{\phi_h^n - \phi_h^{n-1} \circ X_{1h}^n}{\Delta t}, \psi_h \right) + \nu(\nabla \phi_h^n, \nabla \psi_h) = (f^n, \psi_h), \quad \forall \psi_h \in V_h. \tag{9}$$

We show that the integration $(\phi_h^{n-1} \circ X_{1h}^n, \psi_h)$ can be calculated exactly.

At first we prepare two lemmas. The next lemma on the mapping (3) is proved in [14].

Lemma 2 ([14, Proposition 1]) *Suppose*

$$w \in W_0^{1,\infty}(\Omega)^d \quad \textit{and} \quad \Delta t \, |w|_{1,\infty} < 1. \tag{10}$$

Let $F \equiv X_1(w)$ be the mapping defined in (3). Then, $F : \Omega \to \Omega$ is bijective.

Lemma 3 *Let $K_0, K_1 \in \mathcal{T}_h$ and $F : K_0 \to \mathbb{R}^d$ be linear and one-to-one. Let $E_1 \equiv K_0 \cap F^{-1}(K_1)$ and* meas$(E_1) > 0$. *Then, the following hold.*

(i) E_1 is a polygon ($d = 2$) or a polyhedron ($d = 3$).
(ii) $\phi_h \circ F_{|E_1} \in P_k(E_1), \quad \forall \phi_h \in P_k(K_1)$.

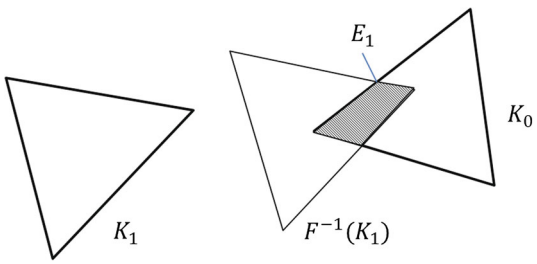

Fig. 1 Elements K_0, K_1 and a polygon E_1

Proof (i) Since both K_0 and $F^{-1}(K_1)$ are triangles ($d = 2$) or tetrahedra ($d = 3$), the intersection is a polygon or a polyhedron. See Fig. 1.

(ii) $F \in P_1(K_0)^d$ implies that $F \in P_1(E_1)^d$ and it holds that $F(E_1) \subset K_1$. Hence, $\phi_h \circ F_{|E_1}$ is well defined and $\phi_h \circ F_{|E_1} \in P_k(E_1)$. □

Proposition 1 *Let ϕ_h, $\psi_h \in V_h$, $w \in W_0^{1,\infty}(\Omega)$ and $X_{1h} \equiv X_1(\Pi_h^{(1)} w)$, where X_1 is the operator defined in (3). Suppose $\alpha_* \Delta t\, |w|_{1,\infty} < 1$. Then, $\int_\Omega (\phi_h \circ X_{1h}) \psi_h dx$ is exactly computable.*

Proof It is sufficient to show that $\int_{K_0} (\phi_h \circ X_{1h}) \psi_h dx$ can be computable exactly for any $K_0 \in \mathcal{T}_h$. The mapping $X_{1h} : \bar{\Omega} \to \Omega$ is bijective since we can apply Lemma 2 thanks to

$$\Delta t |\Pi_h^{(1)} w|_{1,\infty} \le \alpha_* \Delta t |w|_{1,\infty} < 1. \tag{11}$$

Let $\Lambda(K_0) \equiv \left\{ l;\, K_0 \cap X_{1h}^{-1}(K_l) \neq \emptyset \right\}$ and $E_l \equiv K_0 \cap X_{1h}^{-1}(K_l)$ for $l \in \Lambda(K_0)$. Noting that

$$\bigcup_{l \in \Lambda(K_0)} E_l = K_0 \cap \bigcup_{l \in \Lambda(K_0)} X_{1h}^{-1}(K_l) = K_0$$

and that $\mathrm{meas}(E_l \cap E_m) = 0$ for $l \neq m$, $l, m \in \Lambda(K_0)$, we can divide the integration on K_0 into the sum of those on E_l for $l \in \Lambda(K_0)$,

$$\int_{K_0} (\phi_h \circ X_{1h}) \psi_h dx = \sum_{l \in \Lambda(K_0)} \int_{E_l} (\phi_h \circ X_{1h}) \psi_h dx.$$

Since Lemma 3 with $F = X_{1h}$ implies that both $\phi_h \circ X_{1h}$ and ψ_h are polynomials on E_l, we can execute the exact integration. □

Remark 3 In the case of $d = 2$, Priestley [13] approximated $X(t^{n-1}; x, t^n)$ by

$$\widetilde{X}_{1h}(x) = B_1 \lambda_1(x) + B_2 \lambda_2(x) + B_3 \lambda_3(x), \ x \in K_0$$

on each $K_0 \in \mathcal{T}_h$, where $B_i = X(t^{n-1}; A_i, t^n)$, $\{A_i\}_{i=1}^3$ are vertices of K_0 and $\{\lambda_i\}_{i=1}^3$ are the barycentric coordinates of K_0 with respect to $\{A_i\}_{i=1}^3$. Since $\widetilde{X}_{1h}(x)$ is linear in K_0, the decomposition

$$\int_{K_0} (\phi_h \circ \widetilde{X}_{1h}) \psi_h dx = \sum_{l \in \Lambda(K_0)} \int_{E_l} (\phi_h \circ \widetilde{X}_{1h}) \psi_h dx,$$

$$\Lambda(K_0) \equiv \left\{ l;\, K_0 \cap \widetilde{X}_{1h}^{-1}(K_l) \neq \emptyset \right\}, \ E_l \equiv K_0 \cap \widetilde{X}_{1h}^{-1}(K_l)$$

makes the exact integration possible. However, $B_i = X(t^{n-1}; A_i, t^n)$ are the solutions of a system of ordinary differential equations and they cannot be solved exactly in general. In practice, some numerical method, e.g., Runge–Kutta method, is required, which introduces another error.

4 Main results

We show the main results, the stability and convergence of Scheme GSLG.

Hypothesis 1 (i) $u \in C((W_0^{1,\infty})^d)$, (ii) $u \in C((W_0^{1,\infty} \cap W^{2,\infty})^d)$.

Hypothesis 2 $\phi \in H^1(H^{k+1}) \cap Z^2$.

Hypothesis 3 The time increment Δt satisfies $0 < \Delta t \leq \Delta t_0$, where

$$\Delta t_0 \equiv \frac{\delta_*}{\alpha_* \, |u|_{C(W^{1,\infty})}}, \tag{12}$$

and α_* and δ_* are the constants stated in Lemma 1 (Sect. 3) and Lemma 5 (Sect. 5), respectively.

Hypothesis 4 There exists a positive constant c_P such that, for $\psi \in H^{k+1}(\Omega) \cap H_0^1(\Omega)$,

$$\|\widehat{\psi}_h - \psi\|_0 \leq c_P h^{k+1} \, \|\psi\|_{k+1} \, , \tag{13}$$

where $\widehat{\psi}_h$ is the Poisson projection defined in (4).

Remark 4 (i) It is well-known that the H^1-estimate

$$\|\widehat{\psi}_h - \psi\|_1 \leq c_P h^k \, \|\psi\|_{k+1} \tag{14}$$

holds without any specific condition. On the other hand, Hypothesis 4 holds, for example, if Ω is convex, by Aubin-Nitsche Lemma [5].

(ii) Hypothesis 2 implies $\phi \in C(H^{k+1})$ and $\phi^0 \in H^{k+1}(\Omega)$.

Theorem 1 *Suppose Hypotheses 1-(i) and 3. Then, there exists a positive constant c_* independent of h, Δt, ν, ϕ and f such that*

$$\|\phi_h\|_{\ell^\infty(L^2)} + \sqrt{\nu} \, \|\nabla \phi_h\|_{\ell^2(L^2)} \leq c_* \left(\left\| \phi_h^0 \right\| + \|f\|_{\ell^2(L^2)} \right).$$

Theorem 2 *Suppose Hypotheses 1-(ii), 2 and 3.*

(i) There exists a positive constant c_* independent of h, Δt, ν and ϕ such that

$$\begin{aligned} \|\phi - \phi_h\|_{\ell^\infty(L^2)} \quad & + \sqrt{\nu} \, \|\nabla(\phi - \phi_h)\|_{\ell^2(L^2)} \\ & \leq c_* \Bigg\{ \Delta t \, \|\phi\|_{Z^2} + h^k \Bigg(\left\| \frac{\partial \phi}{\partial t} \right\|_{L^2(H^{k+1})} + \|\phi\|_{\ell^\infty(H^{k+1})} \\ & \qquad + \|\phi\|_{\ell^2(0,N_T;H^{k+1})} \Bigg) + h^2 \, \|\nabla \phi\|_{\ell^2(0,N_T-1;L^2)} \Bigg\}. \end{aligned} \tag{15}$$

(ii) There exists a positive constant c_{**} independent of h, Δt, ϕ (but dependent on $1/\nu$) such that

$$\|\phi - \phi_h\|_{\ell^\infty(H^1)} \le c_{**}\left\{\Delta t\,\|\phi\|_{Z^2} + h^k\left(\left\|\frac{\partial\phi}{\partial t}\right\|_{L^2(H^{k+1})} + \|\phi\|_{\ell^\infty(H^{k+1})} + \|\phi\|_{\ell^2(0,N_T-1;H^{k+1})}\right) + h^2\,\|\nabla\phi\|_{\ell^2(0,N_T-1;L^2)}\right\}. \tag{16}$$

(iii) Moreover, suppose Hypothesis 4. Then, there exists a positive constant c_{***} independent of h, Δt, ν and ϕ such that

$$\|\phi - \phi_h\|_{\ell^\infty(L^2)} \le c_{***}\left\{\Delta t\,\|\phi\|_{Z^2} + h^{k+1}\left(\left\|\frac{\partial\phi}{\partial t}\right\|_{L^2(H^{k+1})} + \|\phi\|_{\ell^\infty(H^{k+1})} + \nu^{-1/2}\,\|\phi\|_{\ell^2(0,N_T-1;H^{k+1})}\right) + h^2\,\|\nabla\phi\|_{\ell^2(0,N_T-1;L^2)}\right\}. \tag{17}$$

Remark 5 From Theorem 2, we have

$$\|\phi - \phi_h\|_{\ell^\infty(L^2)} \le c(\Delta t + h^2 + h^k), \qquad c\left(\Delta t + h^2 + \frac{1}{\sqrt{\nu}}h^{k+1}\right)$$
$$\|\phi - \phi_h\|_{\ell^\infty(H^1)} \le c\left(\frac{1}{\nu}\right)(\Delta t + h^2 + h^k).$$

In the case of P_k-element, $k = 1, 2$, the estimate (15) shows the optimal L^2-convergence rate $O(\Delta t + h^k)$ independent of ν. The dependency on ν in (16) and (17) is also inevitable in Scheme LG.

5 Proofs of main theorems

We recall some results used in proving main theorems. For their proofs we only show outlines or refer to the bibliography.

Lemma 4 ([14, Lemma 1]) *Suppose $w \in W_0^{1,\infty}(\Omega)^d$ and*

$$\Delta t\,|w|_{1,\infty} < 1. \tag{18}$$

Let $F \equiv X_1(w)$ be the mapping defined in (3). Then, there exists a positive constant $c(|w|_{1,\infty})$ such that for $\psi \in L^2(\Omega)$

$$\|\psi \circ F\| \le (1 + c\Delta t)\,\|\psi\|.$$

The proof is given in [14].

Lemma 5 *There exists a constant $\delta_* \in (0,1)$ such that, for $w \in W_0^{1,\infty}(\Omega)^d$ and Δt satisfying $\Delta t\,|w|_{1,\infty} \le \delta_*$,*

$$\frac{1}{2} \le \left| \frac{\partial X_1(w)}{\partial x} \right| \le \frac{3}{2},$$

where $|\partial X_1(w)/\partial x|$ is the Jacobian of the mapping $X_1(w)$ defined in (3).

Lemma 5 is easily proved by the fact,

$$\left(\frac{\partial X_1(w)}{\partial x} \right)_{ij} = \delta_{ij} - \Delta t\, \frac{\partial w_i}{\partial x_j}.$$

Lemma 6 *Let $w_i \in W_0^{1,\infty}(\Omega)^d$ and $F_i \equiv X_1(w_i)$ be the mapping defined in (3) for $i = 1, 2$. Under the condition $\Delta t\,|w_i|_{1,\infty} \le \delta_*$, $i = 1, 2$, we have for $\psi \in H^1(\Omega)$*

$$\|\psi \circ F_1 - \psi \circ F_2\| \le \sqrt{2}\Delta t\, \|w_1 - w_2\|_{0,\infty}\, \|\nabla \psi\|.$$

Lemma 6 is a direct consequence of [1, Lemma 4.5] and Lemma 5.

Lemma 7 *Let $w \in W_0^{1,\infty}(\Omega)^d$ and $F \equiv X_1(w)$ be the mapping defined in (3). Under the condition $\Delta t\,|w|_{1,\infty} \le \delta_*$, there exists a positive constant $c(\|w\|_{1,\infty})$ such that for $\psi \in L^2(\Omega)$*

$$\|\psi - \psi \circ F\|_{H^{-1}(\Omega)} \le c\Delta t\, \|\psi\|.$$

Lemma 7 is obtained from [6, Lemma 1] and Lemma 5.

Lemma 8 (discrete Gronwall inequality) *Let a_0 and a_1 be non-negative numbers, $\Delta t \in (0, \frac{1}{2a_0}]$ be a real number, and $\{x^n\}_{n\ge 0}$, $\{y^n\}_{n\ge 1}$ and $\{b^n\}_{n\ge 1}$ be non-negative sequences. Suppose*

$$\frac{x^n - x^{n-1}}{\Delta t} + y^n \le a_0 x^n + a_1 x^{n-1} + b^n, \quad \forall n \ge 1.$$

Then, it holds that

$$x^n + \Delta t \sum_{i=1}^{n} y^i \le \exp\{(2a_0 + a_1) n \Delta t\} \left(x^0 + \Delta t \sum_{i=1}^{n} b^i \right), \quad \forall n \ge 1.$$

Lemma 8 is shown by using the inequalities

$$\frac{1}{1 - a_0 \Delta t} \le 1 + 2a_0 \Delta t \le \exp(2a_0 \Delta t).$$

Outline of the proof of Theorem 1. We substitute ϕ_h^n into ψ_h in (9). We can apply Lemma 4 with $w = u_h^n$ and $\psi = \phi_h^{n-1}$ by virtue of $\Delta t\,|u_h|_{C(W^{1,\infty})} < 1$. The rest of the proof is similar to [14, Theorem 1]. We, therefore, omit it.

Proof of Theorem 2 We first show the estimate (15). Let

$$e_h \equiv \phi_h - \widehat{\phi}_h, \ \eta \equiv \phi - \widehat{\phi}_h, \tag{19}$$

where $\widehat{\phi}_h$ is the Poisson projection defined in (4). From (1a), (1b) and (9) we have

$$\left(\frac{e_h^n - e_h^{n-1} \circ X_{1h}^n}{\Delta t}, \psi_h \right) + \nu(\nabla e_h^n, \nabla \psi_h) = \sum_{i=1}^{4} (R_i^n, \psi_h) \tag{20}$$

for $\psi_h \in V_h$, where

$$\begin{aligned} R_1^n &\equiv \frac{\partial \phi^n}{\partial t} + u^n \cdot \nabla \phi^n - \frac{\phi^n - \phi^{n-1} \circ X_1^n}{\Delta t}, \\ R_2^n &\equiv \frac{\phi^{n-1} \circ X_{1h}^n - \phi^{n-1} \circ X_1^n}{\Delta t}, \\ R_3^n &\equiv \frac{\eta^n - \eta^{n-1}}{\Delta t}, \quad R_4^n \equiv \frac{\eta^{n-1} - \eta^{n-1} \circ X_{1h}^n}{\Delta t}. \end{aligned} \tag{21}$$

Substituting e_h^n into ψ_h, applying Lemma 4 with $F = X_{1h}^n$ and $\psi = e_h^{n-1}$, and evaluating the first term of the left-hand side as

$$\begin{aligned} \left(\frac{e_h^n - e_h^{n-1} \circ X_{1h}^n}{\Delta t}, e_h^n \right) &\geq \frac{1}{2\Delta t} \left(\left\| e_h^n \right\|^2 - \left\| e_h^{n-1} \circ X_{1h}^n \right\|^2 \right) \\ &\geq \frac{1}{2\Delta t} \left(\left\| e_h^n \right\|^2 - (1 + c_1 \Delta t)^2 \left\| e_h^{n-1} \right\|^2 \right) \\ &= \frac{1}{2\Delta t} \left(\left\| e_h^n \right\|^2 - \left\| e_h^{n-1} \right\|^2 \right) - \frac{c_1}{2} (2 + c_1 \Delta t) \left\| e_h^{n-1} \right\|^2, \end{aligned}$$

we have

$$\begin{aligned} &\frac{1}{2\Delta t} \left(\left\| e_h^n \right\|^2 - \left\| e_h^{n-1} \right\|^2 \right) + \nu \left\| \nabla e_h^n \right\|^2 \\ &\leq c_1 \left\| e_h^{n-1} \right\|^2 + \sum_{i=1}^{4} \frac{1}{4\varepsilon_i} \left\| R_i^n \right\|^2 + \left(\sum_{i=1}^{4} \varepsilon_i \right) \left\| e_h^n \right\|^2, \end{aligned} \tag{22}$$

where $\{\varepsilon_i\}_{i=1}^4$ are positive constants satisfying $\Delta t_0 \leq \frac{1}{4\varepsilon_0}$, $\varepsilon_0 \equiv \sum_{i=1}^4 \varepsilon_i$.

We evaluate R_i, $i = 1, \ldots, 4$. Setting

$$y(x, s) = x + (s - 1)\Delta t \, u^n(x), \quad t(s) = t^{n-1} + s\Delta t,$$

we have

$$\frac{\phi^n - \phi^{n-1} \circ X_1^n}{\Delta t} = \frac{1}{\Delta t} \left[\phi(y(\cdot, s), t(s)) \right]_{s=0}^1,$$

which implies

$$
\begin{aligned}
R_1^n &= \frac{\partial \phi^n}{\partial t} + u^n \cdot \nabla \phi^n - \int_0^1 \left\{ u^n(\cdot) \cdot \nabla \phi + \frac{\partial \phi}{\partial t} \right\} (y(\cdot, s), t(s)) ds \\
&= \Delta t \int_0^1 ds \int_s^1 \left\{ \left(u^n(\cdot) \cdot \nabla + \frac{\partial}{\partial t} \right)^2 \phi \right\} (y(\cdot, s_1), t(s_1)) ds_1 \\
&= \Delta t \int_0^1 s_1 \left\{ \left(u^n(\cdot) \cdot \nabla + \frac{\partial}{\partial t} \right)^2 \phi \right\} (y(\cdot, s_1), t(s_1)) ds_1 .
\end{aligned}
$$

Hence, we have

$$
\begin{aligned}
\| R_1^n \| &\le \Delta t \int_0^1 s_1 \left\| \left\{ \left(u^n(\cdot) \cdot \nabla + \frac{\partial}{\partial t} \right)^2 \phi \right\} (y(\cdot, s_1), t(s_1)) \right\| ds_1 \\
&\le c_0 \sqrt{\Delta t} \, \| \phi \|_{Z^2(t^{n-1}, t^n)} ,
\end{aligned} \tag{23}
$$

where we have used the transformation of independent variables from x to y and s_1 to t, and the estimate $|\partial x / \partial y| \le 2$ by virtue of Lemma 5.

From $\Delta t \, |u|_{C(W^{1,\infty})}$, $\Delta t \, |u_h|_{C(W^{1,\infty})} \le \delta_*$, and Lemmas 1 and 6 it holds that

$$
\left\| R_2^n \right\| \le \sqrt{2} \| \nabla \phi^{n-1} \| \| \Pi_h^{(1)} u^n - u^n \|_{0,\infty} \le c_2 h^2 \left\| \nabla \phi^{n-1} \right\| . \tag{24}
$$

R_3^n is evaluated as

$$
\| R_3^n \| = \left\| \int_0^1 \frac{\partial \eta}{\partial t} (\cdot, t(s)) ds \right\| \le \frac{c_P h^k}{\sqrt{\Delta t}} \left\| \frac{\partial \phi}{\partial t} \right\|_{L^2(t^{n-1}, t^n; H^{k+1})} , \tag{25}
$$

where we have used (14).

From $\Delta t \, |u_h|_{C(W^{1,\infty})} \le \delta_*$ and Lemma 6 it holds that

$$
\left\| R_4^n \right\| \le \sqrt{2} \| \nabla \eta^{n-1} \| \| \Pi_h^{(1)} u^n \|_{0,\infty} \le c_0 h^k \left\| \phi^{n-1} \right\|_{k+1} . \tag{26}
$$

Combining (22)–(26), we have

$$
\begin{aligned}
&\frac{1}{2\Delta t} \left(\left\| e_h^n \right\|^2 - \left\| e_h^{n-1} \right\|^2 \right) + \nu \left\| \nabla e_h^n \right\|^2 \le \varepsilon_0 \left\| e_h^n \right\|^2 + c_1 \left\| e_h^{n-1} \right\|^2 \\
&\quad + c_2 \left\{ \Delta t \, \| \phi \|^2_{Z^2(t^{n-1}, t^n)} + h^4 \left\| \nabla \phi^{n-1} \right\|^2 \right. \\
&\qquad \left. + \frac{h^{2k}}{\Delta t} \left\| \frac{\partial \phi}{\partial t} \right\|^2_{L^2(t^{n-1}, t^n; H^{k+1})} + h^{2k} \left\| \phi^{n-1} \right\|^2_{k+1} \right\} .
\end{aligned}
$$

From Lemma 8 we obtain for $n = 1, \ldots, N_T$

$$\left\|e_h^n\right\|^2 + 2\nu\Delta t \sum_{j=1}^{N_T} \left\|\nabla e_h^j\right\|^2 \le c_2\Bigg(\left\|e_h^0\right\|^2 + \Delta t^2 \left\|\phi\right\|_{Z^2}^2 + h^{2k}\left\|\frac{\partial\phi}{\partial t}\right\|_{L^2(H^{k+1})}^2 + h^{2k}\Delta t \sum_{j=0}^{N_T-1}\left\|\phi^j\right\|_{k+1}^2 + h^4\Delta t\sum_{j=0}^{N_T-1}\left\|\nabla\phi^j\right\|^2\Bigg),$$

which implies (15) by virtue of $e_h^0 = 0$ and the triangle inequalities,

$$\begin{aligned}\|\phi - \phi_h\|_{\ell^\infty(L^2)} &\le \|e_h\|_{\ell^\infty(L^2)} + \|\eta\|_{\ell^\infty(L^2)} \\ &\le \|e_h\|_{\ell^\infty(L^2)} + c_P h^k \left\|\phi\right\|_{\ell^\infty(H^{k+1})}, \\ \|\nabla(\phi - \phi_h)\|_{\ell^2(L^2)} &\le \|\nabla e_h\|_{\ell^2(L^2)} + \|\nabla\eta\|_{\ell^2(L^2)} \\ &\le \|\nabla e_h\|_{\ell^2(L^2)} + c_P h^k \left\|\phi\right\|_{\ell^2(H^{k+1})}.\end{aligned} \tag{27}$$

We show the estimate (16). The Eq. (20) can be rewritten as

$$\frac{1}{\Delta t}(e_h^n - e_h^{n-1}, \psi_h) + \nu(\nabla e_h^n, \nabla\psi_h) = \sum_{i=1}^{5}(R_i^n, \psi_h),$$

where

$$R_5^n \equiv \frac{1}{\Delta t}(e_h^{n-1}\circ X_{1h}^n - e_h^{n-1}).$$

From Lemma 6 it holds that

$$\left\|R_5^n\right\| \le \sqrt{2}\|\nabla e_h^{n-1}\|\|\Pi_h^{(1)}u^n\|_{0,\infty} \le c_0\|\nabla e_h^{n-1}\|.$$

Substituting $\overline{D}_{\Delta t}e_h^n \equiv \frac{1}{\Delta t}(e_h^n - e_h^{n-1})$ into ψ_h, and using (23)–(26) for $R_1, \ldots, R_4$, we have

$$\begin{aligned}\left\|\overline{D}_{\Delta t}e_h^n\right\|^2 + \frac{1}{\Delta t}\left(\frac{\nu}{2}\left\|\nabla e_h^n\right\|^2 - \frac{\nu}{2}\left\|\nabla e_h^{n-1}\right\|^2\right) + \frac{\nu}{2\Delta t}\left\|\nabla(e_h^n - e_h^{n-1})\right\|^2 \\ \le c_2\Bigg\{\Delta t\left\|\phi\right\|_{Z^2(t^{n-1},t^n)}^2 + h^4\left\|\nabla\phi^{n-1}\right\|^2 + \frac{h^{2k}}{\Delta t}\left\|\frac{\partial\phi}{\partial t}\right\|_{L^2(t^{n-1},t^n;H^{k+1})}^2 \\ + h^{2k}\left\|\phi^{n-1}\right\|_{k+1}^2\Bigg\} + \frac{c_0}{\nu}\left(\frac{\nu}{2}\left\|\nabla e_h^{n-1}\right\|^2\right) + \frac{1}{2}\left\|\overline{D}_{\Delta t}e_h^n\right\|^2.\end{aligned}$$

From Lemma 8 we have for $n = 1, \ldots, N_T$

$$\frac{\Delta t}{2}\sum_{j=1}^{N_T}\left\|\overline{D}_{\Delta t}e_h^n\right\|^2 + \frac{\nu}{2}\left\|\nabla e_h^n\right\|^2 \le c_2\exp\left(\frac{c_0 T}{\nu}\right)\Bigg(\left\|\nabla e_h^0\right\|^2 + \Delta t^2\left\|\phi\right\|_{Z^2}^2 + h^{2k}\left\|\frac{\partial\phi}{\partial t}\right\|_{L^2(H^{k+1})}^2 + h^{2k}\Delta t\sum_{j=0}^{N_T-1}\left\|\phi^j\right\|_{k+1}^2 + h^4\Delta t\sum_{j=0}^{N_T-1}\left\|\nabla\phi^j\right\|^2\Bigg),$$

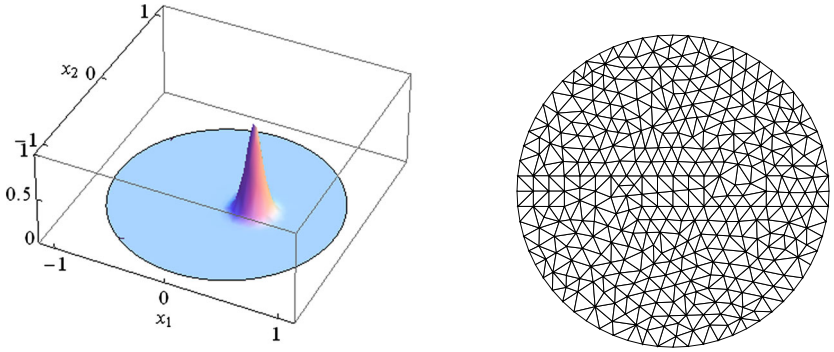

Fig. 2 The function $\phi_e(\cdot, 0)$ (*left*) and the triangulation of $\bar{\Omega}$ for $N = 64$ (*right*) in Example 1

which implies (16) by virtue of $e_h^0 = 0$, the triangle inequality,

$$\begin{aligned}\|\nabla(\phi - \phi_h)\|_{\ell^\infty(L^2)} &\le \|\nabla e_h\|_{\ell^\infty(L^2)} + \|\nabla\eta\|_{\ell^\infty(L^2)} \\ &\le \|\nabla e_h\|_{\ell^\infty(L^2)} + c_P h^k \|\phi\|_{\ell^\infty(H^{k+1})}\end{aligned}$$

and the Poincaré inequality,

$$\|v\|_1 \le c\,\|\nabla v\|\,, \quad \forall v \in H_0^1(\Omega). \tag{28}$$

Now we show the estimate (17). We return to the error Eq. (20). Using (13) in place of (14) in the estimate of R_3^n, we can evaluate (25) as

$$\left\|R_3^n\right\| \le \frac{c_P h^{k+1}}{\sqrt{\Delta t}} \left\|\frac{\partial\phi}{\partial t}\right\|_{L^2(t^{n-1},t^n;H^{k+1})}.$$

From Lemma 7 we have

$$\|R_4^n\|_{H^{-1}(\Omega)} \le c_1 \left\|\eta^{n-1}\right\| \le c_1 h^{k+1} \left\|\phi^{n-1}\right\|_{k+1}.$$

Hence, it holds that

$$(R_4^n, e_h^n) \le \left\|R_4^n\right\|_{H^{-1}(\Omega)} \left\|e_h^n\right\|_1 \le \frac{c_1}{\nu} h^{2(k+1)} \left\|\phi^{n-1}\right\|_{k+1}^2 + \frac{\nu}{2}\left\|\nabla e_h^n\right\|^2,$$

where we have used the Poincaré inequality (28). Using this inequality instead of $\frac{1}{4\varepsilon_4}\left\|R_4^n\right\|^2 + \varepsilon_4\left\|e_h^n\right\|^2$ in (22) and replacing the last term of (27) by $c_P h^{k+1}\|\phi\|_{\ell^\infty(H^{k+1})}$, we obtain (17). □

Table 1 Symbols used in Figs. 3, 6 and 7 and Tables 2–7

X	$\ell^\infty(L^2)$	$\ell^\infty(L^2)$	$\ell^\infty(H_0^1)$
Δt	$O(h^k)$	$O(h^{k+1})$	$O(h^k)$
Scheme LG′	□	⧈	■
Scheme GSLG	○	◎	●

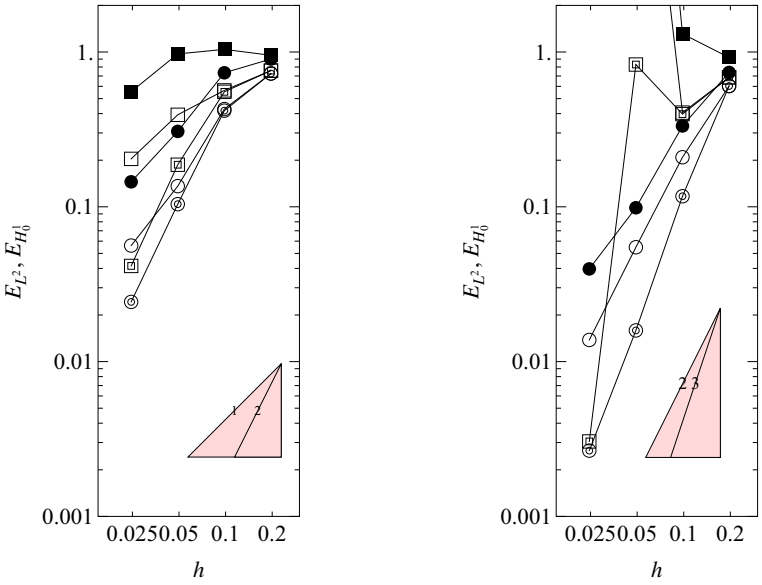

Fig. 3 Graphs of E_{L^2} and $E_{H_0^1}$ versus h in Example 1 by P_k-element. $k = 1$ (*left*) and $k = 2$ (*right*)

6 Numerical results

We show numerical results in $d = 2$. We compare the conventional scheme (Scheme LG′) with the present one (Scheme GSLG). We use FreeFem++ [8] for the triangulation of the domain. Both P_1- and P_2-elements are used. For Scheme LG′ we use the seven points quadrature formula of degree five [7]. A relative error E_X is defined by

$$E_X \equiv \frac{\|\Pi_h^{(k)}\phi - \phi_h\|_{\ell^\infty(X)}}{\|\Pi_h^{(k)}\phi\|_{\ell^\infty(X)}},$$

where $\Pi_h^{(k)}$ is the Lagrange interpolation operator to the P_k-finite element space and $X = L^2(\Omega)$ or $H_0^1(\Omega)$.

Example 1 (*The rotating Gaussian hill* [14]) In (1), Ω is an unit disk, and we set $T = 2\pi$, $\nu = 10^{-5}$,

$$u(x,t) \equiv (-x_2, x_1), \ \ f \equiv 0, \ \ \phi^0 \equiv \phi_e(\cdot, 0),$$

Table 2 The values of errors and orders of the graph in Fig. 3 by P_1-element

N	□	Order	⧈	Oder	■	Order
32	7.58E−01		7.58E−01		9.52E−01	
64	5.65E−01	0.42	5.53E−01	0.45	1.04E+00	−0.13
128	3.93E−01	0.52	1.87E−01	1.56	9.72E−01	0.10
256	2.04E−01	0.95	4.15E−02	2.17	5.54E−01	0.81
N	○	Order	◎	Order	●	Order
32	7.26E−01		7.26E−01		9.01E−01	
64	4.28E−01	0.76	4.18E−01	0.80	7.34E−01	0.30
128	1.36E−01	1.65	1.04E−01	2.01	3.07E−01	1.26
256	5.62E−02	1.27	2.43E−02	2.10	1.45E−01	1.08

Table 3 The values of errors and orders of the graph in Fig. 3 by P_2-element

N	□	Order	⧈	Order	■	order
32	6.86E−01		6.86E−01		9.22E−01	
64	4.06E−01	0.76	3.97E−01	0.79	1.31E+00	−0.51
128	1.67E+02	−8.68	8.30E−01	−1.06	1.72E+03	−10.36
256	1.42E+27	−82.81	3.05E−03	8.09	3.10E+28	−83.90
N	○	Order	◎	Order	●	order
32	6.03E−01		6.03E−01		7.38E−01	
64	2.09E−01	1.53	1.17E−01	2.37	3.33E−01	1.15
128	5.48E−02	1.93	1.59E−02	2.88	9.86E−02	1.76
256	1.38E−02	1.99	2.66E−03	2.58	3.97E−02	1.31

where

$$\phi_e(x,t) \equiv \frac{\sigma}{\sigma+4\nu t}\exp\left\{-\frac{(\bar{x}_1(t)-x_{1,c})^2+(\bar{x}_2(t)-x_{2,c})^2}{\sigma+4\nu t}\right\},$$
$$(\bar{x}_1,\bar{x}_2)(t) \equiv (x_1\cos t + x_2\sin t, -x_1\sin t + x_2\cos t),$$
$$(x_{1,c},x_{2,c}) \equiv (0.25,0),\ \sigma \equiv 0.01.$$

In this problem the identity $\Pi_h^{(1)}u = u$ holds. This problem does not satisfy our setting because Ω is not a polygon and $u \neq 0$ on $\partial\Omega$. The function ϕ_e in Fig. 2 (left) satisfies (1a) and (1c) but does not satisfy the boundary condition (1b). However, we may apply the schemes and treat ϕ_e as the solution since the value of ϕ_e on $\partial\Omega$ is almost equal to zero, less than 10^{-15}, and we may neglect the effect of the boundary value and the term $\int_K(\phi_h^{n-1}\circ X_1^n)\psi_h dx$ and $\int_K(\phi_h^{n-1}\circ X_{1h}^n)\psi_h dx$ on the element K touching the boundary.

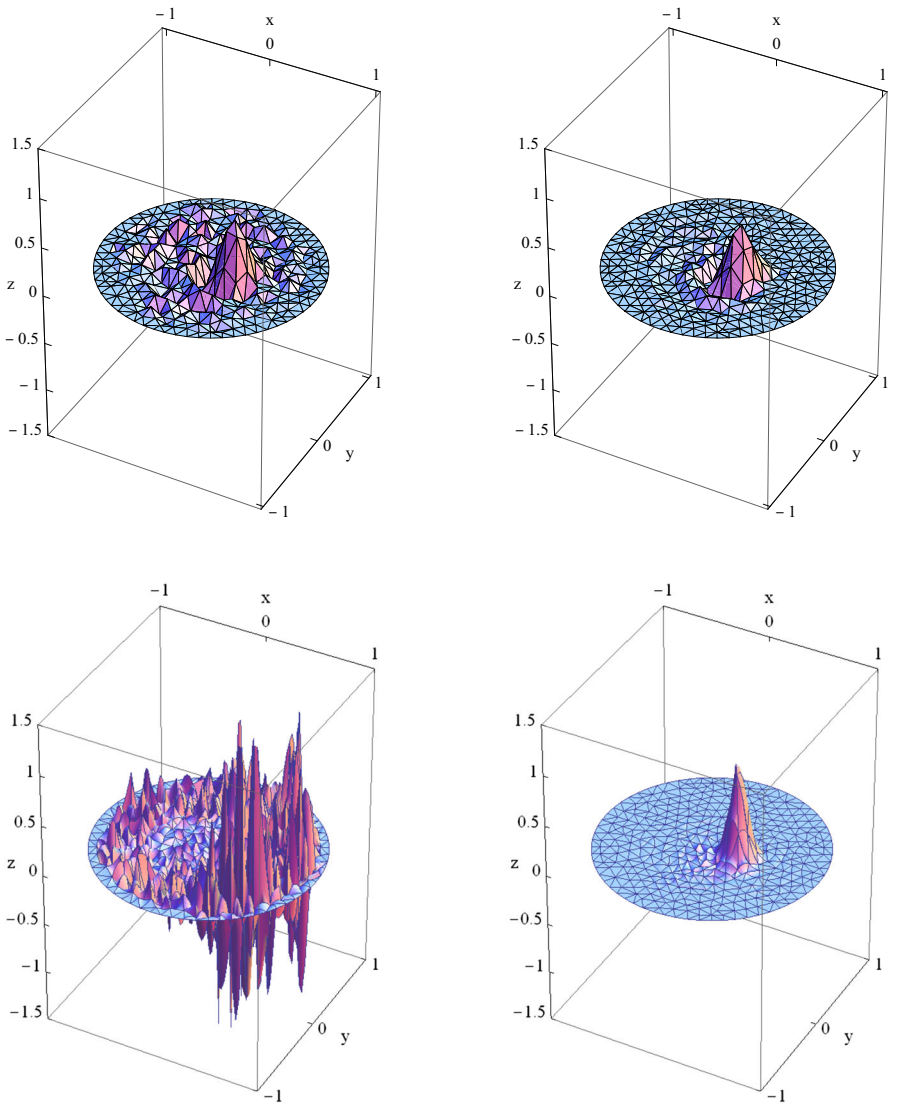

Fig. 4 Solutions ϕ_h^n $(n\Delta t \fallingdotseq 2\pi)$ in Example 1 by Scheme LG′ (*top left*) and Scheme GSLG (*top right*) for P_1-element, and by Scheme LG′ (*bottom left*) and Scheme GSLG (*bottom right*) for P_2-element

Let N be the division number of the circle. We set $h \equiv 2\pi/N$, $N = 32, 64, 128$ and 256. Figure 2 (right) shows the triangulation of $\bar{\Omega}$ for $N = 64$. The time increment Δt is set to be $c_1 h$ and $c_2 h^2$ for P_1-element ($c_1 = \frac{4}{5\pi} \fallingdotseq 0.255$, $c_2 = \frac{64}{5\pi^2} \fallingdotseq 1.30$), $c_3 h^2$ and $c_4 h^3$ for P_2-element ($c_3 = \frac{128}{5\pi^2} \fallingdotseq 2.59$, $c_4 = \frac{2048}{5\pi^3} \fallingdotseq 13.21$) so that we can observe the convergence behavior of $O(h^k)$ for $E_{H_0^1}$, and $O(h^k)$ and $O(h^{k+1})$ for E_{L^2} when P_k-element is employed.

In the following figures we use the symbols shown in Table 1. Figure 3 shows the log-log graphs of E_{L^2} and $E_{H_0^1}$ versus h. The left graph shows the results of P_1-

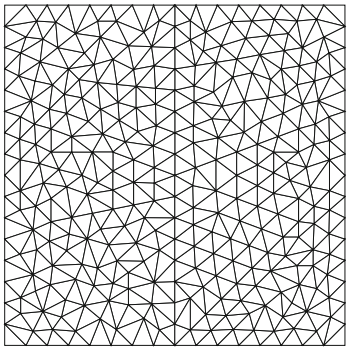

Fig. 5 The triangulation of $\bar{\Omega}$ for $N = 16$ in Example 2

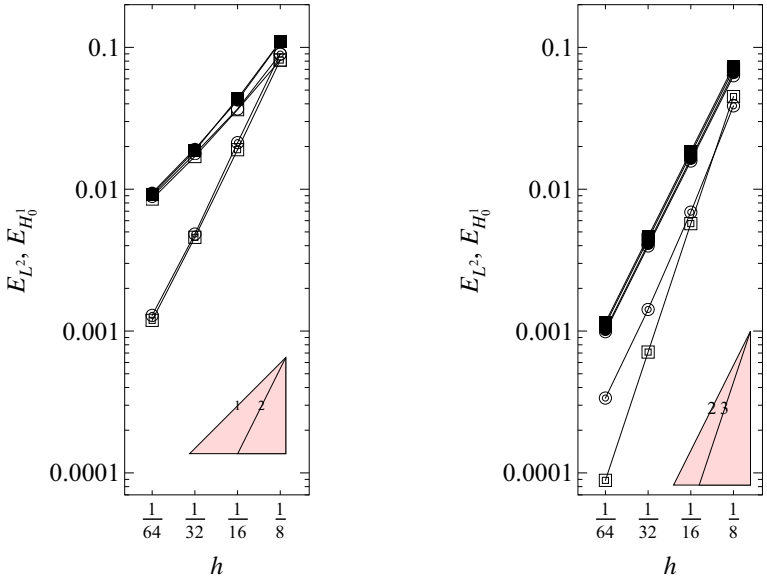

Fig. 6 Graphs of E_{L^2} and $E_{H_0^1}$ versus h in Example 2 with $\nu = 10^{-2}$ by P_k-element. $k = 1$ (*left*) and $k = 2$ (*right*)

element and Table 2 shows the values of them. The convergence order of E_{L^2} with $\Delta t = O(h)$ is less than 1 in Scheme LG′ (□) and more than 1 in Scheme GSLG (◯). The orders of E_{L^2} with $\Delta t = O(h^2)$ are almost 2 for small h in both schemes (⧈, ◎). The convergence of $E_{H_0^1}$ is not observed in Scheme LG′ (■) while the order is almost 1 in Scheme GSLG (●). The right graph of Fig. 3 shows the results of P_2-element and Table 3 shows the values of them. The errors E_{L^2} with $\Delta t = O(h^2)$ are too large at $N = 128$ and 256 to be plotted in the graph in Scheme LG′ (□) while the convergence order is almost 2 in Scheme GSLG (◯). The error E_{L^2} with $\Delta t = O(h^3)$ is large at $N = 128$, but it becomes small again at $N = 256$ in Scheme LG′ (⧈). We will discuss the reason why such a behavior occurs in the forthcoming paper [20]. The order is greater than 2.5 in Scheme GSLG (◎). The errors $E_{H_0^1}$ are too large at $N = 128$ and 256 to be plotted in the graph in Scheme LG′ (■) while we can observe

Table 4 The values of errors and orders of the graph in Fig. 6 by P_1-element

N	□	Order	⧈	Order	■	Order
8	8.14E−02		8.14E−02		1.10E−01	
16	3.64E−02	1.16	1.90E−02	2.10	4.36E−02	1.34
32	1.70E−02	1.10	4.58E−03	2.05	1.87E−02	1.22
64	8.53E−03	0.99	1.19E−03	1.94	9.18E−03	1.03
N	○	Order	◎	Order	●	Order
8	8.97E−02		8.97E−02		1.09E−01	
16	3.68E−02	1.29	2.13E−02	2.07	4.23E−02	1.37
32	1.78E−02	1.05	4.83E−03	2.14	1.92E−02	1.14
64	8.90E−03	1.00	1.29E−03	1.90	9.43E−03	1.03

Table 5 The values of errors and orders of the graph in Fig. 6 by P_2-element

N	□	Order	⧈	Order	■	Order
8	7.01E−02		4.50E−02		7.37E−02	
16	1.77E−02	1.99	5.72E−03	2.98	1.85E−02	1.99
32	4.44E−03	2.00	7.11E−04	3.01	4.63E−03	2.00
64	1.11E−03	2.00	8.86E−05	3.00	1.15E−03	2.01
N	○	Order	◎	Order	●	Order
8	6.31E−02		3.87E−02		6.60E−02	
16	1.58E−02	2.00	6.89E−03	2.49	1.64E−02	2.01
32	3.98E−03	1.99	1.42E−03	2.28	4.12E−03	1.99
64	9.90E−04	2.01	3.37E−04	2.08	1.02E−03	2.01

the convergence of $E_{H_0^1}$ but the order is less than 2 in Scheme GSLG (●). The errors of Scheme GSLG are smaller than those of Scheme LG′ in both cases of P_1- and P_2-element.

Figure 4 shows the solutions ϕ_h^n for $h = 2\pi/64 \fallingdotseq 0.0982$, $\Delta t = 0.0065$, $n\Delta t \fallingdotseq 2\pi$. In the case of P_1-element, the solution of Scheme LG′ is oscillatory while that of Scheme GSLG is much better though a small ruggedness is observed. In the case of P_2-element, the solution of Scheme LG′ is quite oscillatory while that of Scheme GSLG is stable.

Example 2 In (1), Ω is the square $(0, 1) \times (0, 1)$, and we set $T = 1$, $\nu = 10^{-2}$ and 10^{-5},

$$u(x,t) \equiv (\sin \pi x_1 \sin \pi x_2, \sin \pi x_1 \sin \pi x_2), \quad f \equiv \frac{\partial \phi_e}{\partial t} + u \cdot \nabla \phi_e - \nu \Delta \phi_e,$$

$$\phi^0 \equiv \phi_e(\cdot, 0),$$

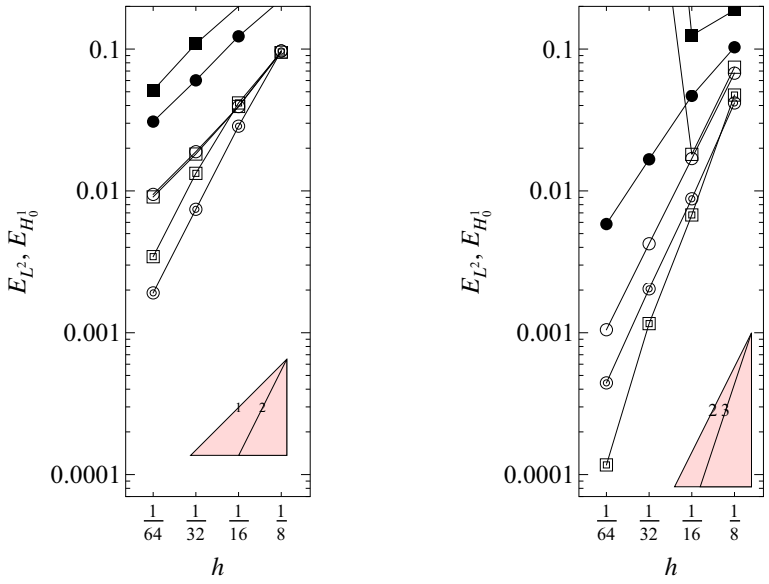

Fig. 7 Graphs of E_{L^2} and $E_{H_0^1}$ versus h in Example 2 with $\nu = 10^{-5}$ by P_k-element. $k = 1$ (*left*) and $k = 2$ (*right*)

Table 6 The values of errors and orders of the graph in Fig. 7 by P_1-element

N	□	Order	⧈	Order	■	Order
8	9.53E−02		9.53E−02		2.90E−01	
16	3.94E−02	1.27	4.17E−02	1.19	2.00E−01	0.54
32	1.82E−02	1.11	1.33E−02	1.65	1.09E−01	0.88
64	9.07E−03	1.00	3.44E−03	1.95	5.12E−02	1.09
N	○	Order	◎	Order	●	Order
8	9.70E−02		9.70E−02		2.23E−01	
16	3.93E−02	1.30	2.86E−02	1.76	1.23E−01	0.86
32	1.89E−02	1.06	7.42E−03	1.95	6.02E−02	1.03
64	9.45E−03	1.00	1.91E−03	1.96	3.08E−02	0.97

where

$$\phi_e(x,t) \equiv \cos(2\pi t)\sin^2(\pi x_1)\sin(2\pi x_2).$$

In this problem, $\Pi_h^{(1)} u \neq u$. Let N be the division number of each side of $\bar{\Omega}$. We set $h \equiv 1/N$, $N = 8, 16, 32$ and 64. Figure 5 shows the triangulation of $\bar{\Omega}$ for $N = 16$. The time increment Δt is set to be $c_1 h$ and $c_2 h^2$ for P_1-element ($c_1 = 0.125, c_2 = 1$), $c_3 h^2$ and $c_4 h^3$ for P_2-element ($c_3 = 1, c_4 = 5.12$) so that we can observe the convergence behavior of $O(h^k)$ for $E_{H_0^1}$, and $O(h^k)$ and $O(h^{k+1})$ for E_{L^2} when P_k-element is employed.

Table 7 The values of errors and orders of the graph in Fig. 7 by P_2-element

N	□	order	⧈	order	■	order
8	7.45E-02		4.74E-02		1.88E-01	
16	1.81E-02	2.04	6.77E-03	2.81	1.25E-01	0.59
32	3.94E+00	−7.77	1.16E-03	2.55	1.22E+02	−9.93
64	1.10E+00	1.84	1.17E-04	3.31	8.17E+01	0.58
N	◯	order	◎	order	●	order
8	6.76E-02		4.17E-02		1.03E-01	
16	1.69E-02	2.00	8.80E-03	2.24	4.68E-02	1.14
32	4.24E-03	1.99	2.04E-03	2.11	1.67E-02	1.49
64	1.05E-03	2.01	4.43E-04	2.20	5.84E-03	1.52

Figure 6 shows the log-log graphs of E_{L^2} and $E_{H_0^1}$ versus h with $\nu = 10^{-2}$. The left graph shows the results of P_1-element and Table 4 shows the values of them. The convergence orders of E_{L^2} with $\Delta t = O(h)$ are almost 1 in both schemes (□, ◯). The orders of E_{L^2} with $\Delta t = O(h^2)$ are almost 2 in both schemes (⧈, ◎). The orders of $E_{H_0^1}$ are almost 1 in both schemes (■, ●). The right graph of Fig. 6 shows the results of P_2-element and Table 5 shows the values of them. The convergence orders of E_{L^2} with $\Delta t = O(h^2)$ are almost 2 in both schemes (□, ◯). The order of E_{L^2} with $\Delta t = O(h^3)$ is almost 3 in Scheme LG′ (⧈) and almost 2 in Scheme GSLG (◎). The orders of $E_{H_0^1}$ are almost 2 in both schemes (■, ●). These results are consistent with the theoretical ones of Scheme GSLG, $E_{L^2} = O(\Delta t + h^2 + h^{k+1})$ and $E_{H_0^1} = O(\Delta t + h^2 + h^k)$.

Figure 7 shows the log-log graphs of E_{L^2} and $E_{H_0^1}$ versus h with $\nu = 10^{-5}$. The left graph shows the results of P_1-element and Table 6 shows the values of them. The convergence orders of E_{L^2} with $\Delta t = O(h)$ are almost 1 in both schemes (□, ◯). The orders of E_{L^2} with $\Delta t = O(h^2)$ are almost 2 for small h in both schemes (⧈, ◎). The orders of $E_{H_0^1}$ are almost 1 in both schemes (■, ●). The right graph of Fig. 7 shows the results of P_2-element and Table 7 shows the values of them. The errors E_{L^2} with $\Delta t = O(h^2)$ are too large at $N = 32$ and 64 to be plotted in the graph in Scheme LG′ (□) while the convergence order is almost 2 in Scheme GSLG (◯). The order E_{L^2} with $\Delta t = O(h^3)$ is almost 3 for small h in Scheme LG′ (⧈) and almost 2 in Scheme GSLG (◎). The errors $E_{H_0^1}$ are too large at $N = 32$ and 64 to be plotted in the graph in Scheme LG′ (■) while we can observe the convergence but the order is less than 2 in Scheme GSLG (●). In order to obtain the theoretical convergence order $O(h^2)$, it seems that finer mesh will be necessary.

7 Conclusions

We have presented a genuinely stable Lagrange–Galerkin scheme for convection-diffusion problems. In the scheme locally linearized velocities are used and the

integration is executed exactly without numerical quadrature. For the P_k-element we have shown error estimates of $O(\Delta t + h^2 + h^{k+1})$ in $\ell^\infty(L^2)$-norm and of $O(\Delta t + h^2 + h^k)$ in $\ell^\infty(H^1)$-norm. We have also obtained error estimate, $c(\Delta t + h^2 + h^k)$ in $\ell^\infty(L^2)$-norm, where the coefficient c is dependent on the exact solution ϕ but independent of the diffusion constant ν. Numerical results have reflected these estimates. The extension to the Navier–Stokes equations will be discussed in a forthcoming paper.

Acknowledgments The first author was supported by JSPS (Japan Society for the Promotion of Science) under Grants-in-Aid for Scientific Research (C)No. 25400212 and (S)No. 24224004 and under the Japanese-German Graduate Externship (Mathematical Fluid Dynamics) and by Waseda University under Project research, Spectral analysis and its application to the stability theory of the Navier–Stokes equations of Research Institute for Science and Engineering. The second author was supported by JSPS under Grant-in-Aid for JSPS Fellows No. 26·964.

References

1. Achdou, Y., Guermond, J.: Convergence analysis of a finite element projection/Lagrange-Galerkin method for the incompressible Navier-Stokes equations. SIAM J. Numer. Anal. **37**(3), 799–826 (2000)
2. Barrett, R., Berry, M., Chan, T.F., Demmel, J., Donato, J., Dongarra, J., Eijkhout, V., Pozo, R., Romine, C., Van der Vorst, H.: Templates for the Solution of Linear Systems: Building Blocks for Iterative Methods, 2nd edn. SIAM, Philadelphia (1994)
3. Bermejo, R., Saavedra, L.: Modified Lagrange-Galerkin methods of first and second order in time for convection-diffusion problems. Numer. Math. **120**(4), 601–638 (2012)
4. Boukir, K., Maday, Y., Métivet, B., Razafindrakoto, E.: A high-order characteristics/finite element method for the incompressible Navier–Stokes equations. Int. J. Numer. Methods Fluids **25**(12), 1421–1454 (1997)
5. Ciarlet, P.G.: The Finite Element Method for Elliptic Problems. Classics in Applied Mathematics. SIAM (2002)
6. Douglas Jr, J., Russell, T.: Numerical methods for convection-dominated diffusion problems based on combining the method of characteristics with finite element or finite difference procedures. SIAM J. Numer. Anal. **19**(5), 871–885 (1982)
7. Hammer, P.C., Marlowe, O.J., Stroud, A.H.: Numerical integration over simplexes and cones. Math. Comput. **10**, 130–137 (1956)
8. Hecht, F.: New development in FreeFem++. J. Numer. Math. **20**(3–4), 251–265 (2012)
9. Morton, K.W., Priestley, A., Suli, E.: Stability of the Lagrange-Galerkin method with non-exact integration. Modél. Mathémat. Anal. Numér. **22**(4), 625–653 (1988)
10. Notsu, H., Tabata, M.: Error estimates of a pressure-stabilized characteristics finite element scheme for the Oseen equations. J. Sci. Comput. (2015). doi:10.1007/s10915-015-9992-8
11. Pironneau, O.: On the transport-diffusion algorithm and its applications to the Navier–Stokes equations. Numer. Math. **38**, 309–332 (1982)
12. Pironneau, O., Tabata, M.: Stability and convergence of a Galerkin-characteristics finite element scheme of lumped mass type. Int. J. Numer. Methods Fluids **64**(10–12), 1240–1253 (2010)
13. Priestley, A.: Exact projections and the Lagrange-Galerkin method: a realistic alternative to quadrature. J. Comput. Phys. **112**(2), 316–333 (1994)
14. Rui, H., Tabata, M.: A second order characteristic finite element scheme for convection-diffusion problems. Numer. Math. **92**, 161–177 (2002)
15. Saad, Y.: Iterative Methods for Sparse Linear Systems. SIAM, Philadelphia (2003)
16. Süli, E.: Convergence and nonlinear stability of the Lagrange-Galerkin method for the Navier-Stokes equations. Numer. Math. **53**(4), 459–483 (1988)
17. Tabata, M.: Discrepancy between theory and real computation on the stability of some finite element schemes. J. Comput. Appl. Math. **199**(2), 424–431 (2007)
18. Tabata, M., Fujima, S.: Robustness of a characteristic finite element scheme of second order in time increment. In: Computational Fluid Dynamics 2004, pp. 177–182. Springer (2006)

19. Tanaka, K., Suzuki, A., Tabata, M.: A characteristic finite element method using the exact integration. Annu. Rep. Res. Inst. Inf. Technol. Kyushu Univ. **2**, 11–18 (2002). (in Japanese)
20. Uchiumi, S.: Conditional stability of the Lagrange-Galerkin scheme with numerical quadrature. JSIAM Lett. (to appear)